Turkish Journal of Electrical Engineering & Computer Sciences

http://journals.tubitak.gov.tr/elektrik/

Research Article

Turk J Elec Eng & Comp Sci
(2022) 30: 2031 – 2043

doi:10.55730/1300-0632.3922

Error analysis of SISO and dual-branch communications with generalized Gaussian noise over FTR fading channels

Mehmet BİLİM*
Department of Electrical and Electronics Engineering, Nuh Naci Yazgan University, Kayseri, Turkey

Received: 01.11.2021 • **Accepted/Published Online:** 02.06.2022 • **Final Version:** 28.09.2022

Abstract: In this paper, we present error probability analysis for single-input single-output (SISO) and asymmetric dual-branch networks with additive white generalized Gaussian noise (AWGGN) over millimeter-wave (mmW) fluctuating two-ray (FTR) fading channels. Then, we examine the error probability evaluation of a SISO system with imperfect phase errors over mmW FTR fading channels. The probability density function (PDF) approach is employed for the error probability performance evaluation and the novel PDF of the asymmetric dual-branch system over Nakagami-m/mmW FTR fading channels is obtained. Specifically, closed-form expressions are derived for the error probability of the SISO and asymmetric dual-branch networks. The derived error expressions facilitate in effectively evaluating the performance of considered networks in the presence of AWGGN and imperfect phase noise with optimal fading parameters and modulation type. The theoretical derivations are extensively confirmed through exact simulations.

Key words: Millimeter-wave communication, fluctuating two-ray fading channels, additive white generalized Gaussian noise, imperfect phase errors

1. Introduction

Millimeter-wave (mmW) communication networks have reached much popularity as a potential candidate for the next generation wireless systems [1–3]. Very high data rates (Gbps data transfer rates) and low latency wireless services are expected to be transmitted in new generation wireless communication systems. For this reason, it is foreseen that mmW communication systems can provide the required bandwidth. In the literature, many researchers have turned to mmW and this subject is popularly studied [4–17]. In [4], a single-port and layer dual-band (DB) antenna using a high frequency level was developed for mmW applications. In [5], the authors proposed the analog precoding schemes for mmW networks by using the dominant vector approaching searching technique. The study in [6] was proposed an array design of a stationary point-to-point mmW network including two links between the transmitter-receiver. A fastlink which is an effective mmW initial access protocol employing the narrowest possible beams was proposed and so, the maximum possible beamforming profit was provided in [7]. The study in [8] focused energy harvesting for sub-6 GHz and mmW hybrid communication systems. An efficient-gain DB resonant cavity antenna for the next generation mmW technology was demonstrated [9]. Wang and Zou proposed a new algorithm, has low computational complexity, for the mmWave massive multiple-input multiple-output networks [10]. In another study [11], the achievable rate and the energy efficiency of analog, digital, and hybrid combining for mmW receiver types were examined. While uplink performance analysis was studied for mmW network with clustered consumers in [12], the average

*Correspondence: mbilim@nny.edu.tr

symbol error rate analysis of rectangular and cross quadrature amplitude modulation for mmW communication systems was comprehensively analyzed [13]. In [14], the performance analysis of mmW transmission with selection combining over fluctuating two-ray (FTR) channels based on moment generating function approach was analyzed. The authors in [15] proposed the alternative statistical characterization evaluation of two-wave with diffuse power (TWDP) for mmW communication and they performed the error probability of TWDP channels. In [16], based on the maximum ratio combining technique, a comprehensive performance evaluation over the FTR channels was presented. Secrecy outage probability and average secrecy capacity analysis for the mmW single-input single-output (SISO) FTR channels were analyzed [17].

On the other hand, the Gaussian distribution uses to characterize for many situations for wireless communication applications. On the contrary to this, the non-Gaussian noise distributions are needed to shape noise sources in many implementations such as some indoor and outdoor wireless environments, ultrawide bandwidth systems, multiuser interference, spectrum sensing, undersea communications, and power line communications [18–21]. Additive white generalized Gaussian noise (AWGGN) encompasses these desirable noise types. Consequently, AWGGN and Laplacian distribution which is a special case of AWGGN, have emerged as a powerful candidate for effectively defining different noise types and greatly evaluating the transmission performance of the mentioned communication systems [22–27]. Additionally, imperfect phase errors emerge as another important issue to be addressed for practical wireless communication applications [28–30]. In [28], the error rate performance of different subcarrier phase-shift keying systems with phase errors was presented. In [29], the error rate analysis of M-ary phase-shift keying (M-PSK) in the presence of phase error was carried out. The author in [30] presented the unified error performance of PSK modulation over mmW wireless channels with imperfect phase errors. This study considered extended generalized-K distribution as fading channel.

Inspired by mmW communication and AWGGN distribution properties, the SISO and asymmetric mmW dual-branch networks with AWGGN and imperfect phase errors which combines these interesting topics are proposed. To the best of authors' knowledge, there is no study for examining the error analysis of SISO mmW communication and an asymmetric dual-branch systems with AWGGN and imperfect phase errors when the literature review is investigated. Firstly, the purpose of this paper is to investigate the theoretical error probability of a SISO communication system with AWGGN over mmW FTR fading channels[1]. Second, an asymmetric dual-branch system over Nakagami-m/mmW FTR fading is studied. Then, the error probability analysis of a SISO system with imperfect phase errors over mmW FTR fading channels is examined. The main contributions of this paper are the derivation of closed-form expressions and the evaluation of the error probability of the considered systems under different conditions. We consider different modulation level for PSK signalling such as binary PSK (BPSK), quadrature PSK (QPSK), and 8-PSK. For each modulation type, we investigate and evaluate the impact of fading parameters (K and m) on the performance of considered systems with AWGGN and imperfect phase errors. So far, there is no study that analyzes SISO and asymmetric dual-branch systems in presence of AWGGN and imperfect phase errors over mmW FTR fading channels.

2. System and channel models

We consider three different network scenarios such as SISO with AWGGN, asymmetric dual-branch, and SISO with imperfect phase erros systems. While the SISO network experiences mmW FTR fading channels, the

[1]A part of this study was presented in URSITR2021 and this presented paper is given in [31]. In [31], only the AWGGN analysis of the SISO mmW FTR channel was presented. Dual-branch and imperfect phase error analyzes are not available.

asymmetric dual-branch system has Nakagami-m/mmW FTR fading channels. Although the studies in [14–17] are related to FTR and mmW communication, asymmetric dual-branch, AWGGN and imperfect phase errors scenarios for FTR channels discussed in this study are not discussed. For this reason, these scenarios are examined for the first time in the literature in this study. The difference in fading of different branches in the dual-branch system is due to the fact that it is a situation that can be encountered in real-life scenarios. Namely in practice, channels between transmitter and receiver nodes may have different fading depending on obstacles or conditions in the environment. For example, in the dual-branch scenario in this study, one branch is assumed to have mmW transmission, while the other is considered to have Nakagami-m fading, one of the conventional fading channel models. Therefore, it is considered appropriate to investigate asymmetric fading in the second scenario.

For the first scenario, the probability density function (PDF) of the instantaneous SNR, γ, of the mmW FTR fading channels is given as [32]

$$\begin{aligned} f_{\gamma}(\gamma) = {} & \frac{1}{2^{m-1}} \frac{1+K}{\bar{\gamma}} \left(\frac{m}{\sqrt{(m+K)^2 - K^2\Delta^2}} \right)^{m} \sum_{q=0}^{\lfloor (m-1)/2 \rfloor} (-1)^q C_q^{m-1} \left(\frac{m+K}{\sqrt{(m+K)^2 - K^2\Delta^2}} \right)^{m-1-2q} \\ & \times \Phi_2^{(4)} \left(1+2q-m,\ m-q-\frac{1}{2},\ m-q-\frac{1}{2},\ 1-m;\ 1; \right. \\ & \left. -\frac{m(1+K)}{(m+K)\bar{\gamma}}\gamma, -\frac{m(1+K)}{(m+K(1+\Delta))\bar{\gamma}}\gamma, -\frac{m(1+K)}{(m+K(1-\Delta))\bar{\gamma}}\gamma, -\frac{(1+K)}{\bar{\gamma}}\gamma \right), \end{aligned} \tag{1}$$

where m is the Nakagami-m variable. While K represents the ratio of the average power of the dominant components to the power of the remaining other paths, Δ is a parameter which depends on the average received powers of the reflective components. $\bar{\gamma}$ is the average SNR and it is defined by $\bar{\gamma} = (E_b/N_0)\, 2\sigma^2 (1+K)$. E_b is the energy per bit and N_0 is the noise term and σ^2 is the variance for the channel noise. $\Phi_2^{(4)}(\cdot)$ is the confluent hypergeometric function. $\lfloor \cdot \rfloor$ is the floor function and C_q^n is a special coefficient and it is expressed as

$$C_q^n = \begin{pmatrix} n \\ q \end{pmatrix} \begin{pmatrix} 2n-2q \\ n \end{pmatrix} = \frac{(2n-2q)!}{q!\,(n-q)!\,(n-2q)!}. \tag{2}$$

In the study in [32], mathematical modeling of the FTR channel was made, and the analyzes in the presented study were not given. As can be seen from Equation (1) and the following definitions, the PDF expression of the mmW FTR channel is mathematically very inconvenient. Therefore, this PDF expression in [33] has been reworked and presented in a mathematically simpler form. For this reason, we prefer to use the PDF expression of the mmW FTR channel in the study presented in [33], as in many studies in the literature. Then the PDF expression in Equation (1) can be rewritten as

$$f_{\gamma}(\gamma) = \frac{m^m}{\Gamma(m)} \sum_{k=0}^{\infty} \frac{K^k \zeta_k \gamma^k}{k!\Gamma(k+1)\,(2\sigma^2)^{k+1}}\, e^{-\frac{\gamma}{2\sigma^2}}, \tag{3}$$

where $\Gamma(\cdot)$ is the Gamma function and

$$\xi_k = \sum_{h=0}^{\infty} \binom{k}{h} \left(\frac{\Delta}{2}\right)^h \sum_{s=0}^{h} \binom{h}{l} \Gamma(k+m+2s-h)\, e^{\frac{\pi(2s-h)i}{2}} \times \left((m+K)^2 - (K\Delta)^2\right)^{-\frac{(k+m)}{2}} P_{k+m-1}^{h-2s}\left((m+K)/\sqrt{(m+K)^2-(K\Delta)^2}\right), \tag{4}$$

where $P_j^i(\cdot)$ is the first-order Legendre function [34, Eq. (8.702)].

For the second scenario, since a dual-branch system Nakagami-m/mmW FTR asymmetric structure is considered, the PDF expression for the first transmission branch is expressed as

$$f_{\gamma_1}(\gamma) = \left(\frac{m_1}{\bar{\gamma}_1}\right)^{m_1} \frac{\gamma^{m_1-1}}{\Gamma(m_1)} e^{-\frac{m_1}{\bar{\gamma}_1}\gamma}. \tag{5}$$

The PDF expression for the second transmission branch from (3) is given as

$$f_{\gamma_2}(\gamma) = \frac{{m_2}^{m_2}}{\Gamma(m_2)} \sum_{j=0}^{\infty} \frac{K_2^j \xi_{j,2} \gamma^j}{j!\Gamma(j+1)(2\sigma^2)^{j+1}}\, e^{-\frac{\gamma}{2\sigma^2}}. \tag{6}$$

The total PDF expression for the dual-branch system is written as [32, Eq. (4)], [36, Eq. (5)]

$$f_{\gamma_{SC}}(\gamma) = f_{\gamma_1}(\gamma) F_{\gamma_2}(\gamma) + f_{\gamma_2}(\gamma) F_{\gamma_1}(\gamma), \tag{7}$$

where $F_\gamma(\gamma)$ is the cumulative distribution function (CDF) and it is defined by

$$F_\gamma(\gamma) = \int_0^\gamma f_\gamma(\gamma)\, d\gamma. \tag{8}$$

Substituting (5) and (6) into (8) and utilizing [34, Eq. (3.381.1)], the CDF expressions for the first and second transmission branch is obtained as

$$F_{\gamma_1}(\gamma) = Q\left(\frac{m_1}{\bar{\gamma}_1}\right)^{-m_1} \gamma\left(m_1, \frac{m_1}{\bar{\gamma}_1}\gamma\right) \tag{9}$$

$$F_{\gamma_2}(\gamma) = M \sum_{j=0}^{\infty} Z\left(\frac{1}{2\sigma^2}\right)^{-(j+1)} \gamma\left(j+1, \frac{1}{2\sigma^2}\gamma\right), \tag{10}$$

where $\gamma(\cdot,\cdot)$ is the lower incomplete Gamma function. $Q = \left(\frac{m_1}{\bar{\gamma}_1}\right)^{-m_1} \frac{1}{\Gamma(m_1)}$, $M = \frac{{m_2}^{m_2}}{\Gamma(m_2)}$ and $Z = \frac{K_2^j \xi_{j,2}}{j!\Gamma(j+1)(2\sigma^2)^{j+1}}$. By inserting (9), (10), (5) and (6) in (7), the total PDF expression of the Nakagami-m/mmW

FTR asymmetric dual-branch system is derived as

$$f_{\gamma_{SC}}(\gamma) = QM\sum_{j=0}^{\infty} Z\left(\frac{1}{2\sigma^2}\right)^{-(j+1)} \gamma^{m_1-1} e^{-\frac{m_1}{\bar{\gamma}_1}\gamma}\gamma\left(j+1, \frac{1}{2\sigma^2}\gamma\right) + QM\sum_{j=0}^{\infty} Z\left(\frac{1}{2\sigma^2}\right)^{-(j+1)} \left(\frac{m_1}{\bar{\gamma}_1}\right)^{-m_1} \gamma^{j} e^{-\frac{\gamma}{2\sigma^2}}\gamma\left(m_1, \frac{m_1}{\bar{\gamma}_1}\gamma\right). \tag{11}$$

3. Theoretical analysis

Error probability, P_e can be mathematically evaluated by

$$P_e = \int_0^{\infty} P(e|\gamma) f_{\gamma}(\gamma) d\gamma, \tag{12}$$

where $P(e|\gamma)$ is the conditional error probability expression and it is defined by $P(e|\gamma) = AQ_z\left(\sqrt{B\gamma}\right)$. A and B are modulation parameters. For example, $A = 1$ and $B = 2$ for BPSK and $A = 2$ and $B = 1$ for QPSK. Here, $Q_z(\cdot)$ is the generalized Gaussian function and it is expressed as

$$Q_z(t) = \frac{z{\Lambda_0}^{2/z}}{2\Gamma(1/z)} \int_t^{\infty} e^{-\Lambda_0^z y^z} dy, \tag{13}$$

where $\Lambda_0 = \sqrt{\Gamma(3/z)/\Gamma(1/z)}$ and z is a parameter that specifies the type of noise. The noise types according to the z values are given in [27 and 37, Table I]. By using the expression in (13), $P(e|\gamma)$ is rewritten as

$$P(e|\gamma) = \frac{Az{\Lambda_0}^{2/z}}{2\Gamma(1/z)} \int_{\sqrt{B\gamma}}^{\infty} e^{-\Lambda_0^z y^z} dy. \tag{14}$$

Mathematically, using the expression $P(e|\gamma)$ in (14) does not seem very useful to reach the solution. For this reason, it has been thought to use the expression presented in [27], which has a very tight approximation of the expression $P(e|\gamma)$ and simplifies the mathematical solution process. This approximation has been used in many studies and yielded successful results [25–27], [37]. Accordingly, the expression given in (14) is presented again as follows:

$$P(e|\gamma) \approx A\sum_{g=1}^{4} \tau_g e^{-\varepsilon_g B\gamma}, \tag{15}$$

where τ_g and ε_g are the parameters of the approximation and the values of these parameters are given in [27 and 37, Table III].

For the first scenario, substituting (15), (3) into (12) and changing the order of the integral, we have

$$P_e^1 \approx A\frac{m^m}{\Gamma(m)} \sum_{g=1}^{4} \tau_g \sum_{k=0}^{\infty} \frac{K^k \xi_k}{k!\Gamma(k+1)(2\sigma^2)^{k+1}} \int_0^{\infty} \gamma^k e^{-\gamma\left(\frac{1}{2\sigma^2}+\varepsilon_g B\right)} d\gamma\,. \tag{16}$$

Then utilizing [34, Eq. (3.381.4)], the P_e for a SISO mmW FTR system is derived as

$$P_e^1 \approx A\frac{m^m}{\Gamma(m)}\sum_{g=1}^{4}\tau_g\sum_{k=0}^{\infty}\frac{K^k\xi_k}{k!(2\sigma^2)^{k+1}}\left(\frac{1}{2\sigma^2}+\varepsilon_g B\right)^{-(k+1)}. \tag{17}$$

For the second scenario, plugging (11) and (15) in (12), we get

$$\begin{aligned} P_e^2 \approx A\sum_{g=1}^{4}\tau_g\Bigg\{&\int_0^{\infty} e^{-\varepsilon_g B\gamma}QM\sum_{j=0}^{\infty}Z\left(\frac{1}{2\sigma^2}\right)^{-(j+1)}\gamma^{m_1-1}e^{-\frac{m_1}{\bar{\gamma}_1}\gamma}\gamma\left(j+1,\frac{1}{2\sigma^2}\gamma\right)d\gamma \\ &+\int_0^{\infty} e^{-\varepsilon_g B\gamma}QM\sum_{j=0}^{\infty}Z\left(\frac{1}{2\sigma^2}\right)^{-(j+1)}\left(\frac{m_1}{\bar{\gamma}_1}\right)^{-m_1}\gamma^{j}e^{-\frac{\gamma}{2\sigma^2}}\gamma\left(m_1,\frac{m_1}{\bar{\gamma}_1}\gamma\right)d\gamma\Bigg\}. \end{aligned} \tag{18}$$

After some mathematical manipulations, the expression in (18) is rewritten as

$$P_e^2 \approx A\sum_{g=1}^{4}\tau_g\left\{I_1+I_1\right\}, \tag{19}$$

where

$$I_1 = QM\sum_{j=0}^{\infty}Z\left(\frac{1}{2\sigma^2}\right)^{-(j+1)}\int_0^{\infty}\gamma^{m_1-1}e^{-\left(\frac{m_1}{\bar{\gamma}_1}+\varepsilon_g B\right)\gamma}\gamma\left(j+1,\frac{1}{2\sigma^2}\gamma\right)d\gamma \tag{20}$$

$$I_2 = QM\sum_{j=0}^{\infty}Z\left(\frac{1}{2\sigma^2}\right)^{-(j+1)}\left(\frac{m_1}{\bar{\gamma}_1}\right)^{-m_1}\int_0^{\infty}\gamma^{j}e^{-\gamma\left(\frac{1}{2\sigma^2}+\varepsilon_g B\right)}\gamma\left(m_1,\frac{m_1}{\bar{\gamma}_1}\gamma\right)d\gamma \tag{21}$$

I_1 and I_2 are the same form and using [34, eq. (6.455.2)], I_1 and I_2 are obtained as

$$\begin{aligned} I_1 = QM\sum_{j=0}^{\infty}Z\left(\frac{1}{2\sigma^2}\right)^{-(j+1)}&\frac{\left(\frac{1}{2\sigma^2}\right)^{j+1}\Gamma(m_1+j+1)}{(j+1)\left(\frac{1}{2\sigma^2}+\frac{m_1}{\bar{\gamma}_1}+\varepsilon_g B\right)^{m_1+j+1}} \\ &\times{}_2F_1\left(1,m_1+j+1;j+2;\frac{\left(\frac{1}{2\sigma^2}\right)}{\left(\frac{1}{2\sigma^2}+\frac{m_1}{\bar{\gamma}_1}+\varepsilon_g B\right)}\right) \end{aligned} \tag{22}$$

$$\begin{aligned} I_2 = QM\sum_{j=0}^{\infty}Z\left(\frac{1}{2\sigma^2}\right)^{-(j+1)}\left(\frac{m_1}{\bar{\gamma}_1}\right)^{-m_1}&\frac{\left(\frac{m_1}{\bar{\gamma}_1}\right)^{m_1}\Gamma(m_1+j+1)}{m_1\left(\frac{1}{2\sigma^2}+\frac{m_1}{\bar{\gamma}_1}+\varepsilon_g B\right)^{m_1+j+1}} \\ &\times{}_2F_1\left(1,m_1+j+1;m_1+1;\frac{\left(\frac{m_1}{\bar{\gamma}_1}\right)}{\left(\frac{1}{2\sigma^2}+\frac{m_1}{\bar{\gamma}_1}+\varepsilon_g B\right)}\right), \end{aligned} \tag{23}$$

where ${}_2F_1\left(\cdot,\cdot;\cdot;\cdot\right)$ is the Gauss hypergeometric function. After inserting (22) and (23) in (19), we derived as

$$P_e^2 \approx A\sum_{g=1}^{4}\tau_g\left\{QM\sum_{j=0}^{\infty}Z\left(\frac{1}{2\sigma^2}\right)^{-(j+1)}\frac{\left(\frac{1}{2\sigma^2}\right)^{j+1}\Gamma\left(m_1+j+1\right)}{(j+1)\left(\frac{1}{2\sigma^2}+\frac{m_1}{\bar{\gamma}_1}+\varepsilon_g B\right)^{m_1+j+1}}\right.$$
$$\times{}_2F_1\left(1,m_1+j+1;j+2;\frac{\left(\frac{1}{2\sigma^2}\right)}{\left(\frac{1}{2\sigma^2}+\frac{m_1}{\bar{\gamma}_1}+\varepsilon_g B\right)}\right)QM\sum_{j=0}^{\infty}Z\left(\frac{1}{2\sigma^2}\right)^{-(j+1)} \tag{24}$$
$$\left.\times\left(\frac{m_1}{\bar{\gamma}_1}\right)^{-m_1}\frac{\left(\frac{m_1}{\bar{\gamma}_1}\right)^{m_1}\Gamma\left(m_1+j+1\right)}{m_1\left(\frac{1}{2\sigma^2}+\frac{m_1}{\bar{\gamma}_1}+\varepsilon_g B\right)^{m_1+j+1}}{}_2F_1\left(1,m_1+j+1;m_1+1;\frac{\left(\frac{m_1}{\bar{\gamma}_1}\right)}{\left(\frac{1}{2\sigma^2}+\frac{m_1}{\bar{\gamma}_1}+\varepsilon_g B\right)}\right)\right\}.$$

In this study, the imperfect phase errors case for a SISO system over FTR channel as another scenario is considered. Therefore, by utilizing [38], the $P\left(e|\,\gamma\right)$ expression for M-PSK signalling is given as

$$P\left(e\,|\gamma\right)=1-\frac{1}{\sqrt{2\pi\sigma_a^2}}\int_{-\pi/M}^{\pi/M}e^{\left(\frac{-a^2}{2\sigma_a^2}\right)}da$$
$$=1-erf\left(\Theta\sqrt{\gamma}\right)=erfc\left(\Theta\sqrt{\gamma}\right), \tag{25}$$

where M is the modulation level for M-PSK modulation, a is the total angular deviation of the received signal, σ_a is variance and it is define as $\sigma_a^2=\frac{1}{2\gamma}+\frac{1}{\delta\gamma}$. $\Theta=\frac{(\pi/M)}{\sqrt{\left(1+\frac{2}{\delta}\right)}}$ and δ is the multiplication factor for the first-order phase-lock-loop which employs for the the phase error estimation in the receiver side. By substituting (3), (25) into (12), we have

$$P_e^3=\frac{m^m}{\Gamma\left(m\right)}\sum_{k=0}^{\infty}\frac{K^k\xi_k}{k!\Gamma\left(k+1\right)\left(2\sigma^2\right)^{k+1}}\int_0^{\infty}erfc\left(\Theta\sqrt{\gamma}\right)\gamma^k e^{-\frac{\gamma}{2\sigma^2}}d\gamma. \tag{26}$$

By changing $\gamma=t^2$, the expression in (26) is rewritten as

$$P_e^3=\frac{m^m}{\Gamma\left(m\right)}\sum_{k=0}^{\infty}\frac{2K^k\xi_k}{k!\Gamma\left(k+1\right)\left(2\sigma^2\right)^{k+1}}\int_0^{\infty}t^{2k+1}e^{-\frac{t^2}{2\sigma^2}}erfc\left(\Theta t\right)dt. \tag{27}$$

After some mathematical manipulations and by employing [39, Eq. (2.8.5.6)], the error probability expression of a SISO system with imperfect phase errors over FTR fading channels is derived as

$$P_e^3=\frac{m^m}{\Gamma\left(m\right)}\sum_{k=0}^{\infty}\frac{2K^k\xi_k}{k!\Gamma\left(k+1\right)\left(2\sigma^2\right)^{k+1}}\left\{\frac{-\Theta}{\sqrt{\pi}\left(\frac{1}{2\sigma^2}\right)^{k+1.5}}\;\Gamma\left(k+1.5\right)\right.$$
$$\left.\times{}_2F_1\left(0.5,k+1.5;1.5;\frac{-\Theta^2}{\left(\frac{1}{2\sigma^2}\right)}\right)+\frac{\Gamma\left(k+1\right)}{2\left(\frac{1}{2\sigma^2}\right)^{k+1}}\right\}. \tag{28}$$

4. Asymptotic analysis

The asymptotic of the P_e for the first scenario at high average SNR region, $P_e^{1,\infty}$, can be deduced after $\bar{\gamma} \to \infty$ as

$$P_e^{1,\infty} = A\frac{m^m}{\Gamma(m)}\sum_{g=1}^{4}\tau_g\sum_{k=0}^{\infty}\frac{K^k\xi_k}{k!(2\sigma^2)^{k+1}}(\varepsilon_g B)^{-(k+1)}. \tag{29}$$

If we invoke as $k=1$ in (29), $P_e^{1,\infty}$ can be obtained as

$$P_e^{1,\infty} = A\frac{m^m}{\Gamma(m)}\sum_{g=1}^{4}\tau_g\frac{K\xi_1}{(2\sigma^2\varepsilon_g B)^2}. \tag{30}$$

Following the same steps for $P_e^{1,\infty}$, the asymptotic of the P_e for the second scenario at high average SNR region ($\bar{\gamma} \to \infty$), $P_e^{2,\infty}$, can be evaluated as

$$\begin{aligned} P_e^{2,\infty} \approx A\sum_{g=1}^{4}\tau_g\Bigg\{ & QMZ\left(\frac{1}{2\sigma^2}\right)^{-2}\frac{\left(\frac{1}{2\sigma^2}\right)^2\Gamma(m_1+2)}{2\left(+\frac{m_1}{\bar{\gamma}_1}+\varepsilon_g B\right)^{m_1+2}} \\ & \times QMZ\left(\frac{1}{2\sigma^2}\right)^{-(2)}\times\left(\frac{m_1}{\bar{\gamma}_1}\right)^{-m_1}\frac{\left(\frac{m_1}{\bar{\gamma}_1}\right)^{m_1}\Gamma(m_1+2)}{m_1\left(\frac{m_1}{\bar{\gamma}_1}+\varepsilon_g B\right)^{m_1+2}}\Bigg\}. \end{aligned} \tag{31}$$

5. Numerical results

In this section, we present numerical results to confirm our theoretical framework in previous sections. A comprehensive investigation is illustrated on the impact of the fading severity parameters of links and different modulation types on the error probability of considered network scenarios with AWGGN noise ($z = 1$ and Laplacian noise) and imperfect phase errors. While the error probability curves of the SISO communication over mmW FTR channels are presented in Figures 1 and 2, the error probabilities of the Nakagami-m/mmW FTR asymmetric dual-branch system in Figures 3–5 are also studied. Furthermore, the error probability performance evaluation of the SISO system with imperfect phase errors is presented in Figure 6. For Figures 1, 2, 6 and 3–5 the number of channels are 1 and 2, respectively. For all figures, the upper limit of the infinity summation for the expressions in (17), (24), and (28) is 20 terms. Tables 1 and 2 present the results of evaluating the error probability expressions at a certain upper limit. From Tables 1 and 2, it is seen that the first 20 terms for the error probability calculation is quietly enough.

Figure 1 shows the error probability of the considered SISO network versus the average SNR for various channel fading severity parameters. A and B modulation parameters for QPSK are set to 2 and 1, respectively. mmW FTR channel parameters are set as $K = 15$ and $\Delta = 0.5$. The solid and dashed lines indicate our analytical and asymptotic results, and the circle symbols represent the exact simulation results. From Figure 1, we can see that our analytical and asymptotic results match well with the exact simulation results, which affirms our theoretical analysis. The error probability performance changes with the increase or decrease of the fading severity parameters. This is because the mmW FTR fading channel represents different fading conditions by changing fading parameters (m) as mentioned before.

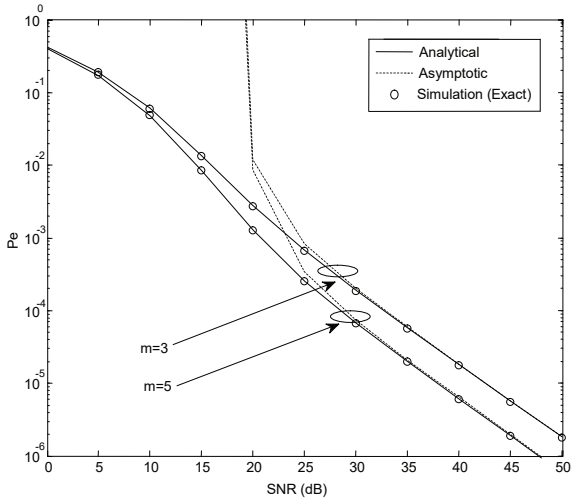

Figure 1. Error probability of the SISO system over mmW FTR fading channels with different fading parameters.

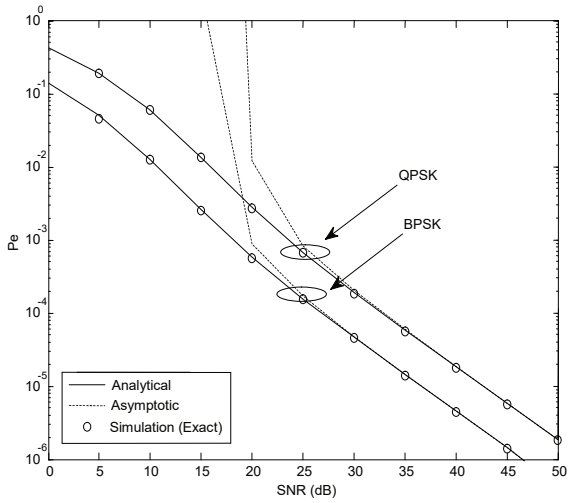

Figure 2. Error probability of the SISO system over mmW FTR fading channels with different modulations.

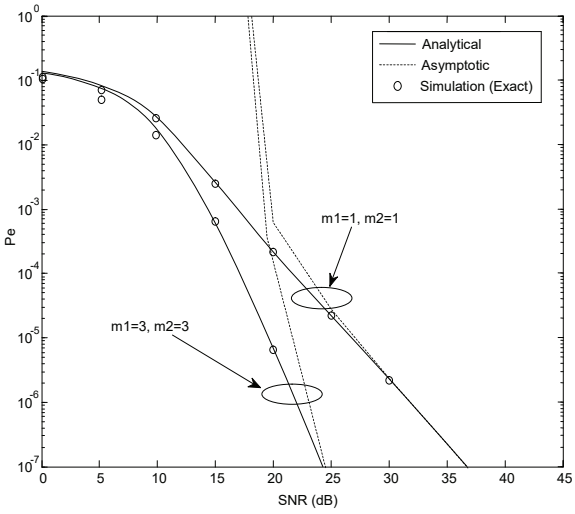

Figure 3. Error probability of an asymmetric dual-branch system with different fading parameters.

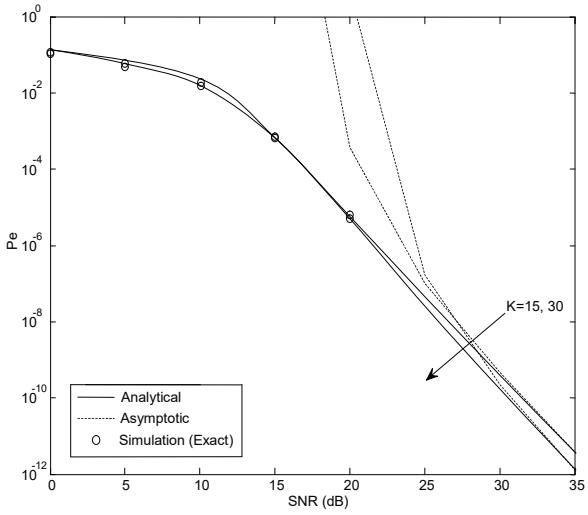

Figure 4. Error probability of an asymmetric dual-branch system with different K values.

Figure 2 gives the error probability performance of a SISO network for different modulation schemes. m, K and Δ are set to 3, 15, and 0.5, respectively. It shows that when the order of modulation level increases, the error probability performance decreases in the whole SNR regions (low, medium, and high). This means the error probability of a SISO network with BPSK modulation gets better than the error probability of the considered system with QPSK modulation in the Laplacian noise scenario, as expected. With BPSK modulation, the overall error probability performance of the considered system is 10^{-3} at $SNR \approx 18\,\text{dB}$. On the other hand, the error probability level of 10^{-3} is obtained at $SNR \approx 23\,\text{dB}$ for the SISO system with QPSK modulation. Again, from these results, we can observe that the error probability is very close to the exact simulation one in different modulation schemes. It is indicated that our error probability expression can be used to effectively evaluate the error probability performance of the considered network in all SNR regions.

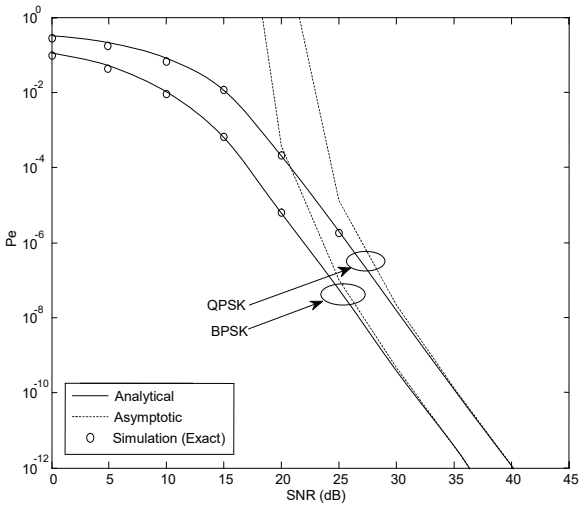

Figure 5. Error probability of an asymmetric dual-branch system with different modulation schemes.

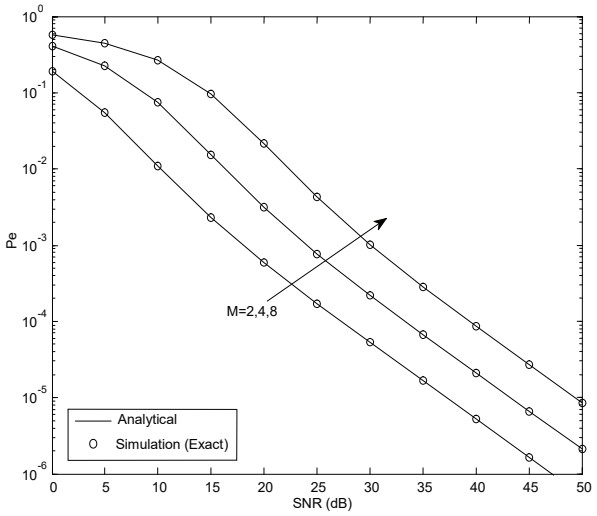

Figure 6. Error probability of a SISO system with imperfect phase errors over FTR fading channels.

Table 1. Values of the error probability of SISO system with AWGGN and imperfect phase errors over mmW FTR fading channels for different levels of truncation ($K = 15,\ \Delta = 0.5,\ m = 3,\ z = 1$, and $\bar{\gamma} = 30dB$ for SISO system with AWGGN and $K = 15,\ \Delta = 0.5,\ m = 3,\ \delta = 2,\ M = 8$, and $\bar{\gamma} = 30dB$ for SISO system with imperfect phase noise).

Upper limit	Analytical expression Eq. (17)	Analytical expression Eq. (28)
1	**0.0000467**638	**0.00**0948574
5	**0.0000468**271	**0.00100**7820
10	**0.0000468**33	**0.00100**8270
15	**0.0000468**655	**0.00100**8854
20	**0.0000468651**	**0.001008870**
30	**0.0000468651**	**0.001008870**

Table 2. Values of the error probability of the Nakagami-m/mmW FTR asymmetric dual-branch system with AWGGN for different levels of truncation ($m_1 = 3,\ K = 15,\ \Delta = 0.5,\ m_2 = 3,\ z = 1$, and $\bar{\gamma} = 30dB$).

Upper limit	Analytical expression Eq. (24)
1	$\mathbf{1.}20185 \times 10^{-8}$
5	$\mathbf{1.3}6998 \times 10^{-8}$
10	$\mathbf{1.37}693 \times 10^{-8}$
15	$\mathbf{1.3755}1 \times 10^{-8}$
20	$\mathbf{1.37545} \times 10^{-8}$
30	$\mathbf{1.37545} \times 10^{-8}$

Figure 3 demonstrates the error probability of a Nakagami-m/mmW FTR asymmetric dual-branch system with different fading parameters. We set $K = 10,\ \Delta = 0.5,\ A = 1,\ B = 2$ (BPSK), $\bar{\gamma}_1 = \bar{\gamma}_2 = \frac{\bar{\gamma}}{2}$ and $\bar{\gamma}_1 + \bar{\gamma}_2 = \bar{\gamma}$. It shows that the error probability has a parallel behavior with fading parameter. To illustrate, $m_1 = m_2 = 3$ gains more effective for the error probability performance compared with $m_1 = m_2 = 1$. In other

words, an important effect of increasing the values of the fading parameter m_1 and m_2 is clearly appeared on the error probability over whole SNR values.

Figure 4 shows the second investigation of the error probability performance for an asymmetric dual-branch system when the different values of the K parameter for the mmW FTR fading channel. Again, we set to $20th$ term for the upper bound of the infinity summations expressions, $m_1 = m_2 = 3$, $\Delta = 0.5$, $A = 1$, $B = 2$ (BPSK), $\bar{\gamma}_1 = \bar{\gamma}_2 = \frac{\bar{\gamma}}{2}$ and $\bar{\gamma}_1 + \bar{\gamma}_2 = \bar{\gamma}$. It is expected that less error probability with increasing K values can be attained at high SNR values. However, it can be said that the increasing K parameter value generally plays a minor effect on the error probability performance.

Figure 5 demonstrates the error probability of an asymmetric dual-branch system using different modulations. The assigned fading parameters in this figure are considered as $m_1 = m_2 = 3$, $\Delta = 0.5$, $K = 15$, $\bar{\gamma}_1 = \bar{\gamma}_2 = \frac{\bar{\gamma}}{2}$ and $\bar{\gamma}_1 + \bar{\gamma}_2 = \bar{\gamma}$. As it can be seen from that figure, the modulation types play a major role in enhancing the error probability performance. Overall, better error probability performance is attained over the BPSK modulation for all SNR regime. From Figures 1–5, it is clearly seen that the analytical and asymptotic results obtained by the derived error probability expressions were confirmed by the exact simulations and were indicated to be good matching. Moreover, it is clear that the variation of the m parameter in mmW FTR channels affects the error probability more than the variation of the K parameter. The reason for this is that the increasing of m parameter value reduces the fluctuation for mmW FTR channels. Against this, a high value of K stands for the total energy of the dominant components is larger than the total energy of the scattered waves. Changes of the modulation level also have an effect on the considered system models like each communication systems.

Finally, Figure 6 illustrates the impact of different modulation levels, M, of M-PSK for a SISO system with imperfect phase errors over FTR channels. In this scenario, the parameters have been setup as $m = 3$, $K = 15$, $\Delta = 0.5$, and $\delta = 2$. While M value increases, the error probability performance of the considered system decreases, as expected. Again, it is seen that the analytical results obtained by the proposed expression in (28) are well matches with the exact simulation results.

6. Conclusion

In this paper, we study the error probability performance of a SISO and asymmetric dual-branch networks over FTR fading channels, considering AWGGN and imperfect phase errors. The PDF and closed-form error probability expressions for the considered systems are derived. The theoretical analysis is validated by comprehensive exact numerical simulations. The use of different modulation types and fading parameters are also discussed. Both theoretical and exact simulation results show that the modulation type and the fading severity of the considered systems have a significant impact on the error probability performance.

References

[1] Samsung Research. The Next Hyper-Connected Experience for All. Technical Report, 2021.

[2] Agrawal DP, Zeng Q-A. Introduction to Wireless and Mobile Systems. Hoboken, NJ, USA: Wiley, 2011.

[3] Rappaport TS. Wireless Communication. Chennai, India: Pearson, 2011.

[4] Guo YQ, Pan YM, Zheng SY, Lu K. A Singly-fed dual-band microstrip antenna for microwave and millimeter-wave applications in 5G wireless communication. IEEE Transactions on Vehicular Technology 2021; 70 (6): 5419-5430. doi: 10.1109/TVT.2021.3070807

[5] Wang Y, Zou W, Tao Y. Analog precoding designs for millimeter wave communication systems. IEEE Transactions on Vehicular Technology 2018; 67 (12): 11733-11745. doi: 10.1109/TVT.2018.2874633

[6] Cai W, Wang P, Li Y, Zhang Y, Vucetic B. Deployment optimization of uniform linear antenna arrays for a two-path millimeter wave communication system. IEEE Communications Letters 2015; 19 (4): 669-672. doi: 10.1109/LCOMM.2015.2401570

[7] Aykin I, Krunz M. Efficient beam sweeping algorithms and initial access protocols for millimeter-wave networks. IEEE Transactions on Wireless Communications 2020; 19 (4): 2504-2514. doi: 10.1109/TWC.2020.2965926

[8] Muhammad NA, Seman N, Apandi NIA, Li Y. Energy harvesting in sub-6 GHz and millimeter wave hybrid networks. IEEE Transactions on Vehicular Technology 2021; 70 (5): 4471-4484. doi: 10.1109/TVT.2021.3068956

[9] Wen L, Yu Z, Zhu L, Zhou J. High-gain dual-band resonant cavity antenna for 5G millimeter-wave communications. IEEE Antennas and Wireless Propagation Letters 2021; 20 (10): 1878-1882. doi: 10.1109/LAWP.2021.3098390

[10] Wang Y, Zou W. Low complexity hybrid precoder design for millimeter wave MIMO systems. IEEE Communications Letters 2019; 23(7): 1259-1262. doi: 10.12676/j.cc.2019.02.003

[11] Abbas WB, Cuba FG, Zorzi M. Millimeter wave receiver efficiency: a comprehensive comparison of beamforming schemes with low resolution ADCs. IEEE Transactions on Wireless Communications 2017; 6 (12): 8131-8146. doi: 10.1109/TWC.2017.2757919

[12] Muhammad NA, Apandi NIA, Li Y, Seman N. Uplink performance analysis for millimeter wave cellular networks with clustered users. IEEE Transactions on Vehicular Technology 2020; 69 (6): 6178-6188. doi: 10.1109/TVT.2020.2980291

[13] Bilim M,Kapucu N. Average symbol error rate analysis of QAM schemes over millimeter wave fluctuating two-ray fading channels. IEEE Access 2019; 7 (1): 105746-105754. doi: 10.1109/ACCESS.2019.2932147

[14] Al-Hmood H, Al-Raweshidy HS. Performance analysis of mmWave communications with selection combining over fluctuating-two ray fading model. IEEE Communications Letters 2021; 25(8): 2531-2535. doi: 10.1109/LCOMM.2021.3087524

[15] Maric A, Kaljic E, Njemcevic P. An alternative statistical characterization of TWDP fading model. MDPI Sensors 2021; 21 (22): 7513. doi:10.3390/s21227513

[16] Olyaee M, Eslami M, Haghighat J. Performance of maximum ratio combining of fluctuating two-ray (FTR) mmWave channels for 5G and beyond communications. Transaction on Emerging Telecommunication Technology 2019; 30: e3601. doi:10.1002/ett.3601

[17] Zeng W, Zhang J, Chen S, Peppas KP, Ai B. Physical layer security over fluctuating two-ray fading channels. IEEE Transactions on Vehicular Technology 2018; 67 (9): 8949-8953. doi: 10.1109/TVT.2018.2842126

[18] Soury H, Yilmaz F, Alouini M-S. Average bit error probability of binary coherent signaling over generalized fading channels subject to additive generalized Gaussian noise. IEEE Communication Letters 2012; 16(6): 785-788. doi: 10.1109/LCOMM.2012.040912.112612

[19] Beaulieu NC, Young DJ. Designing time-hopping ultrawide bandwidth receivers for multiuser interference environments. Proc. IEEE 2009; 97 (2): 255-284. doi: 10.1109/JPROC.2008.2008782

[20] Chiani M, Giorgetti A. Coexistence between UWB and narrowband wireless communication systems. Proc. IEEE 2009; 97 (2): 231-254. doi: 10.1109/JPROC.2008.2008778

[21] Mathur A, Bhatnagar MR, Panigrahi BK. Performance evaluation of PLC under the combined effect of background and impulsive noises. IEEE Communication Letters 2015; 19 (7): 1117-1120. doi: 10.1109/LCOMM.2015.2429129

[22] Beaulieu NC, Bartoli G, Marabissi D, Fantacci R. The structure and performance of an optimal continuous-time detector for Laplace noise. IEEE Communication Letters 2013; 17 (6): 1065-1068. doi: 10.1109/LCOMM.2013.042313.130164

[23] Thompson MW, Chang H-S. Coherent detection in Laplace noise. IEEE Transactions on Aerospace and Electronic Systems 1994; 30 (2): 452-461. doi: 10.1109/7.272267

[24] Shao H, Beaulieu NC. An investigation of block coding for Laplacian noise. IEEE Transactions on Wireless Communications 2012; 11 (7): 2362-2372. doi: 10.1109/TWC.2012.051712.101143

[25] Bilim M. Approximate ASER analysis of MIMO TAS/MRC networks over Weibull fading channels. Annals of Telecommunications 2021; 76:73-81. doi: 10.1007/s12243-020-00810-2

[26] Bilim M. Uplink communications with AWGGN over non-homogeneous fading channels. Physical Communication 2020; 39 (101047): 1-5. doi: 10.1016/j.phycom.2020.101047

[27] Salahat E, Saleh H. Novel unified analysis of orthogonal space-time block codes over generalized-K and AWGGN MIMO networks. In: IEEE 81st Vehicular Technology Conference (VTC Spring); Glasgow, Scotland; 2015; pp. 1-4. doi: 10.1109/VTCSpring.2015.7145958

[28] Song X, Yang F, Cheng J, Al-Dhahir N, Xu Z. Subcarrier phase-shift keying systems with phase errors in lognormal turbulence channels. Journal of Lightwave Technology 2015; 33 (9): 1896-1904. doi: 10.1109/JLT.2015.2398847

[29] Jang Y, Jeong J, Yoon D. Bit error floor of MPSK in the presence of phase error. IEEE Transactions on Vehicular Technology 2016; 65 (5): 3782-3786 doi: 10.1109/TVT.2015.2437792

[30] Khanna H. On the unified error performance of PSK modulation schemes over mm-wave wireless channels affected by carrier phase synchronization errors. International Journal of Communication Systems 2021; 34 (7): e4712. doi:10.1002/dac.4712

[31] Bilim M. Performance analysis of a mmW SISO system with AWGGN over fluctuating two-ray fading channels. In: 10th International Radio-Scientific Union (URSI); Gebze (online), Turkey; 2021; pp. 1-3. (in Turkish with an abstract in English).

[32] Romero-Jerez JM, Lopez-Martinez FJ, Paris JF, Goldsmith AJ. The fluctuating two-ray fading model: statistical characterization and performance analysis. IEEE Transaction on Communication 2017; 16 (7): 4420 4432. doi: 10.1109/TWC.2017.2698445

[33] Zhang J, Zeng W, Li X, Sun Q, Peppas KP. New results on the fluctuating two-ray model with arbitrary fading parameters and its applications. IEEE Transaction on Vehicular Technology 2018; 67 (3): 2766-2770. doi: 10.1109/TVT.2017.2766784

[34] Gradshteyn IS, Ryzhik IM. Table of Integrals, Series and Products. San Diego, CA, USA: Academic, 2007.

[35] Bilim M. Dual-branch SC wireless systems with HQAM for beyond 5G over $\eta - \mu$ fading channels. Peer-to-Peer Networking and Applications 2021; 14: 305-318. doi: 10.1007/s12083-020-00946-x

[36] Khatalin S. Performance of dual-branch selection combining diversity systems in non-identical Nakagami-q (Hoyt) fading channels IET Communications 2010; 4 (5): 585-595. doi: 10.1049/iet-com.2009.0445

[37] Bilim M. Error analyse of generalized Gaussian noise for alternate Rician fading. Nigde Omer Halisdemir Journal Engineering Science 2021; 10 (1): 84-90. (in Turkish with an abstract in English). doi: 10.28948/ngumuh.765657

[38] Gappmair W, Nistazakis HE. Subcarrier PSK performance in terrestrial FSO links impaired by gamma-gamma fading, pointing errors, and phase noise. Journal of Lightwave Technology, 2017; 35 (9): 1624-1632. doi: 10.1109/JLT.2017.2685678

[39] Prudnikov AP, Brychkov YA, Marichev OI. Integrals, and series: special functions (Vol. 2). New York, USA: Gordon and Breach Science, 1986.